Dynamics of structural transitions in liquids

Frank H. Stillinger and Thomas A. Weber
Bell Laboratories, Murray Hill, New Jersey 07974
(Received 2 June 1983)

The "inherent structures" which underlie the liquid state are those stable particle packings (potential minima) which can be reached by a steepest-descent quench on the potential-energy hypersurface. This paper explores the dynamics of transition between distinct inherent structures for a simple classical model of monatomic substances. Molecular-dynamics calculations with 32 and 108 particles have been carried out with running construction of the mapping to potential minima. This determines the distribution of stable packings according to their potential energy and shows how transition rates between alternative structures vary with total system energy. Melting and freezing events have been monitored in this manner. We observe occasional transitions in localized "two-state" (bistable) systems in strongly supercooled amorphous states. Transitions in fluid states display a peculiar intermittency that may have relevance to self-diffusion and viscous flow.

I. INTRODUCTION

Two recent papers have advanced a novel approach to understanding the liquid state and the melting process that produces it.[1,2] The basic idea involved was to separate the statistical problem into two parts, namely, the identification and characterization of the mechanically stable packings of the molecules, followed by an accounting for vibrational motion (generally anharmonic) about those mechanically stable points. That prior work was concerned principally with static equilibrium properties. This paper extends the study into the dynamic regime by examining the transition kinetics between "inherent structures" (i.e., the packings). For this purpose we have carried out some molecular-dynamics calculations on an elementary model for monatomic substances.

Consider an N-particle system in D dimensions subject to periodic boundary conditions, and let $\Phi(\vec{r})$ be the potential energy when the configuration of the N particles is specified by the DN-dimensional vector $\vec{r}$. We will suppose that Φ is differentiable. The inherent structures for this many-body system are given by solutions to

$$\vec{\nabla}\Phi(\vec{r})=0 \; ; \tag{1.1}$$

these form the set of stable packings within which the force on every particle vanishes. The packings will differ in their potential energy, with the expectation that the lowest packing energy involves maximal crystallinity.

With the exception of a few configurations with vanishing measure, every configuration $\vec{r}$ can be assigned uniquely to its own inherent structure, a Φ minimum. The procedure for making this assignment is to move from $\vec{r}$ along the steepest-descent direction on the Φ hyperface until inevitably the relevant minimum is encountered. Steepest-descent paths are solutions to the differential equation

$$\dot{\vec{r}}=-\vec{\nabla}\Phi(\vec{r}) \; . \tag{1.2}$$

By this means the full configuration space of vectors $\vec{r}$ is divided exhaustively into connected regions $\mathscr{R}_\alpha$, $\alpha=1,\ldots,\Omega$, one surrounding each of the Ω configurations at which Φ is a local minimum.

The Newtonian equations of motion (in suitable units for which particle masses are unity) can be written as follows:

$$\ddot{\vec{r}}=-\vec{\nabla}\Phi(\vec{r}) \; , \tag{1.3}$$

to be solved with appropriate initial conditions. As the system vector $\vec{r}(t)$ moves about in the configuration space it will, under most circumstances of interest, move across a sequence of distinguishable regions $\mathscr{R}_\alpha$. The primary concern at present is in the function $\alpha(t)$ which monitors transitions between the quench regions. It is clear that initial conditions for Eq. (1.3) determine whether the function $\alpha(t)$ samples a large number of regions or is trapped forever in just a few.

One expects[2,3] that the number Ω of local Φ minima for large N to be approximately

$$\Omega \simeq N!\exp(\nu N) \; , \tag{1.4}$$

where ν is some positive number. The first factor accounts for particle permutations that yield minima of identical energy. The second factor estimates the number of essentially distinct ways of arranging the particles in stable packings. Results reported below permit a rough estimate to be made for ν for the one specific model system examined.

Section II presents the model, and provides some details about the molecular dynamics simulation technique with which it has been explored. Systems of two sizes have been employed. Section III discusses results for $N=32$, a system small enough that all Φ minima apparently can be enumerated, yet large enough that the crystal-fluid transition is clearly manifested. Section IV presents results for a larger system of $N=108$ particles. For both of these system sizes the temperature dependence of transition rates has been examined. Section V summarizes conclusions and discusses directions for future work.

II. DYNAMICAL MODEL

The Lennard-Jones (LJ) 12-6 pair potential:

$$V_{\mathrm{LJ}}(r)=\epsilon v(r/\sigma)\ , \qquad v(x)=4(x^{-12}-x^{-6})\ , \tag{2.1}$$

has frequently been used to represent interactions in noble-gas systems, such as argon.[4–6] The function v has the following properties:

$$v(1)=0\ , \quad v(2^{1/6})=-1\ , \quad v'(2^{1/6})=0\ . \tag{2.2}$$

From the standpoint of the computer simulation of many-body phenomena, obvious advantage occurs when interactions have strictly limited range. Since this is not the case with V_{LJ}, often this function has been used only to represent interactions below some preassigned cutoff distance R_c, with all interactions of greater range simply ignored.[4,6] The same advantage, however, can be achieved in another way, namely, by considering the following continuous family of functions:

$$v_p(x)=\begin{cases} A(x^{-12}-x^{-p})\exp[(x-a)^{-1}]\ , & 0<x<a \\ 0\ , & x\geq a\ . \end{cases} \tag{2.3}$$

This form automatically satisfies the first of Eqs. (2.2). By insisting that the other two Eqs. (2.2) are also satisfied, the constants A and a can be uniquely determined for each p. Connection to the Lennard-Jones potential is obvious:

$$\lim_{p\to 6-} v_p(x)=v(x)\ . \tag{2.4}$$

Table I presents values calculated for A and a with several selected powers p. In addition to the finite-range advantage that obtains when $p<6$, the exponential factor in v_p causes derivatives of all orders to go continuously to zero as $r\to a$, which tends to improve stability of numerical integration for equations of motion.

Our molecular dynamics study has used v_p with $p=0$ (instead of v with a cutoff), and a cubic unit cell with periodic boundary conditions. Under these circumstances a perfect face-centered cubic array of particles can be created within the system provided that the number of particles has the form

$$N=4n^3\ . \tag{2.5}$$

TABLE I. Parameters for the reduced pair potential v_p defined in Eq. (2.3).

p	A	a	$v_p''(2^{1/6})$
0	8.805 977	1.652 194	67.426
1	8.646 355	1.706 488	64.727
2	8.421 246	1.779 751	62.381
3	8.096 886	1.886 613	60.399
4	7.604 504	2.064 922	58.805
5	6.767 441	2.464 918	57.655
6	4.000 000	∞	57.146

We have examined the two cases $n=2$ and 3 ($N=32$ and 108).

Classical equations of motion have been integrated by a standard fifth-order Gear algorithm,[7] using reduced units in which ϵ, σ, and particle mass m all are unity. In those units the step length employed for integration was

$$\Delta t=0.001\,25\ . \tag{2.6}$$

Dynamical runs typically lasted $10^4\Delta t$; when converted to real time by using ϵ, σ, and m for Ar this interval corresponds to 27 ps.

For all calculations reported below the reduced density was held fixed at

$$\rho=1.0\ . \tag{2.7}$$

This is the density at which nearest neighbors in the perfect fcc structure have separation $2^{1/6}$, and it is extremely close to the density for which the v_0 lattice sum over that structure is at a minimum.

At closely spaced times during execution of the molecular dynamics program the system configuration $\vec{r}(t)$ at that instant is subjected to a quenching operation that locates the relevant minimum $\alpha(t)$. The potential energy of that minimum is then recorded. A conjugate-gradient method[8] has been used for this minimum-location task. By far the larger portion of the required computing time is devoted to this quenching, and it is this fact which thus far has prevented us from investigating substantially larger systems.

Calculations on both system sizes were initiated with particles placed in the regular fcc arrangement, with very small initial velocities. Temperatures were determined as usual from average kinetic energy, and total system energy was varied by homogeneous velocity scaling. Properties of any given state were observed only after elapse of an adequate period of equilibration.

III. 32-PARTICLE SYSTEM

The potential energy per particle

$$\phi=N^{-1}\sum_{j<k} v_0(r_{jk}) \tag{3.1}$$

fluctuates during the temporal evolution of the constant-energy dynamics. Average values determined for this quantity have been plotted against reduced temperature T in Fig. 1 for the 32-particle system. The results fall along two clearly distinguishable branches which, in spite of the small number of particles involved, can be identified as solid- and liquid-phase branches. Transitions between these branches have been observed as sudden events during both heating and cooling stages. Although overlap of the two branches has been shown in the figure to indicate the possibility of superheating and undercooling, we find that transitions between the branches occur in both directions most frequently when $T=2.0\pm 0.2$. We shall informally designate this as the "melting point" for the small system.

While the system is at low temperature and exhibits $\langle\phi\rangle$ values lying on the solid branch in Fig. 1, the steepest-descent quench operation invariably maps the sys-

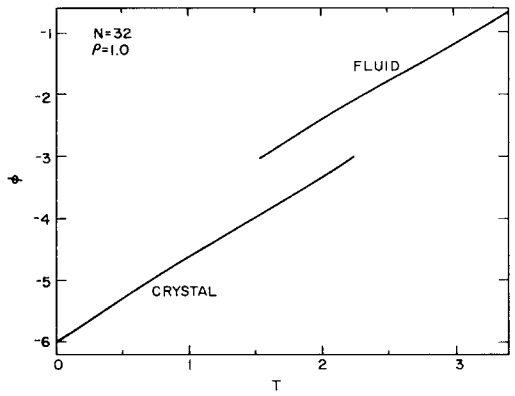

FIG. 1. Mean potential energy per particle vs temperature for the 32-particle system.

tem onto the regular crystalline fcc packing, for which the potential energy per particle is

$$\phi = -6.000\,002\,32\ . \tag{3.2}$$

On account of the finite range of the potential, this same absolute minimum value applies even to the infinite system limit at $\rho = 1$. However, the quench mapping, upon entering the liquid state, produces a different and more interesting pattern. Figure 2 shows the quench values for ϕ computed every ten time steps during a liquid-phase run at $T = 2.337$. Frequent transitions appear between many distinct inherent structures, all of which lie in potential-energy well above the absolute minimum, Eq. (3.2). The figure displays frequent returns to a previously visited ϕ value. It also shows apparent gaps in the distribution of quench potential, most notably between -5.371 and -6.000.

Rates of structural transitions are markedly increased by raising the temperature, as comparison of Figs. 2 and 3 clearly shows. The latter presents quench-ϕ values for a similar molecular dynamics run of 10^4 steps, but for a very hot fluid at $T = 6.440$. The transition rate is now so fast that serious doubt can be raised whether quenching every ten time steps is frequent enough to convey the true complexity of the mapping under study. Note the fact that the crystalline packings at -6.000 were occasionally sampled during this run, revealed by a few crosses at this level. But obviously the available configuration space at this high total energy is dominated by regions belonging to amorphous packings.

The highest value ever observed in the 32-particle system for a quench ϕ is

$$\phi = -4.861\,049\,77\ , \tag{3.3}$$

which corresponds to a "worst" packing geometry at the given density. We cannot absolutely exclude the possibility that an even higher quench-ϕ value might be discovered, but it seems unlikely in view of the extensive nature of our search.

A computer-constructed catalog of the distinct quench-ϕ values was created and updated as the various 32-particle runs were carried out. In this manner 157 distinct packings were discovered with ϕ values in the range indicated by Eqs. (3.2) and (3.3). If this listing is close to complete and if the Ω formula (1.4) approximately de-

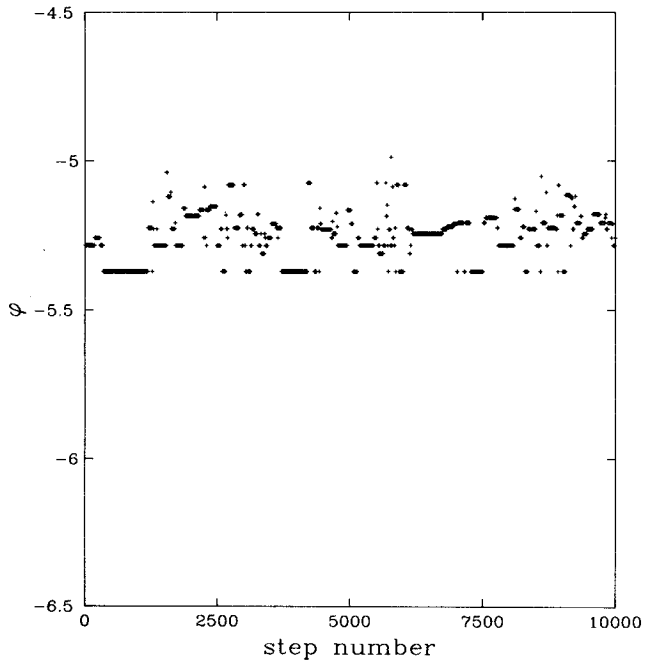

FIG. 2. Quench potential energy per particle during the dynamics of a 32-particle liquid at $T = 2.337$. Individual crosses appear at each ten-step interval.

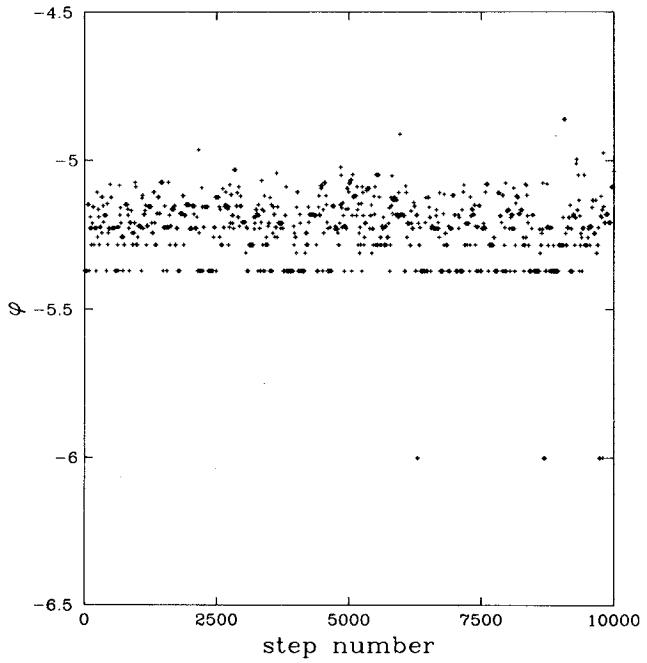

FIG. 3. Quench-ϕ values for a 32-particle fluid at $T = 6.440$, evaluated every ten time steps.

scribes the 32-particle system, then we can estimate the parameter ν:

$$\nu \simeq (\ln 157)/32 \simeq 0.16 \ . \tag{3.4}$$

Figure 4 displays a "melting event" as viewed from the perspective of the quench-ϕ plot. The system had been in one of the crystalline regions at the beginning of the 10^4-step run, and remained there for the first 1210 steps. At this point it discovered an exit channel from this crystalline region to the manifold of amorphous states within which it subsequently remained. The average temperature for the run was 2.070, close to our estimate of the melting point for this small system. We also note in passing that the inverse case, a "freezing event," has also been observed in this temperature range, whereby the system dropped from the amorphous manifold into one of the crystalline minima.

The system can easily be trapped in the amorphous manifold by rapidly cooling the equilibrium fluid through the melting temperature. Figure 5 shows the result of such treatment, producing an amorphous state at $T=0.773$. Quite obviously the transition rate between regions of distinct quench ϕ has declined markedly.

Figure 6 presents the numbers of transitions counted during the course of several 10^4-step runs for the 32-particle system, plotted against temperature. The states with $T>2.0$ are stable fluid states, the others with $T<2.0$ are all supercooled amorphous states. Although considerable scatter is present the overall trend is clear. By fitting these numbers to a simple rate expression of the form

$$KT^{1/2}\exp(-\Delta\Phi/T) \ , \tag{3.5}$$

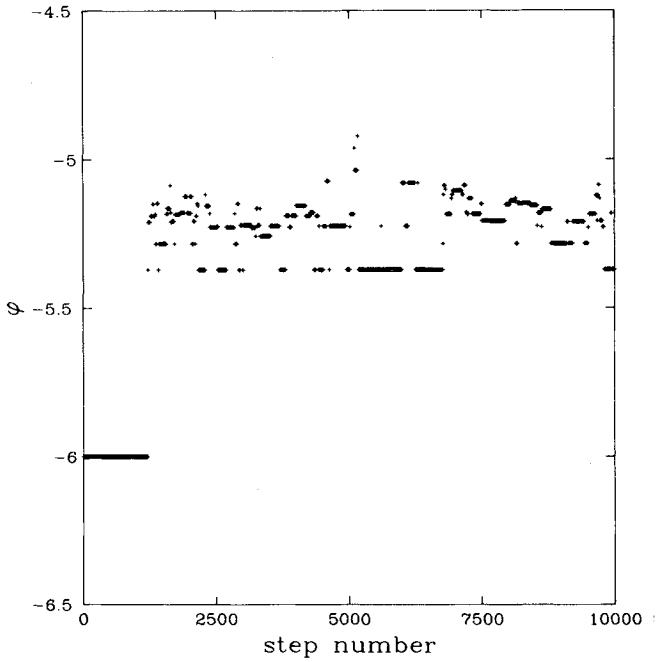

FIG. 4. Melting event for the 32-particle system. Quenches were carried out every ten time steps. Average temperature for this run is $T=2.070$.

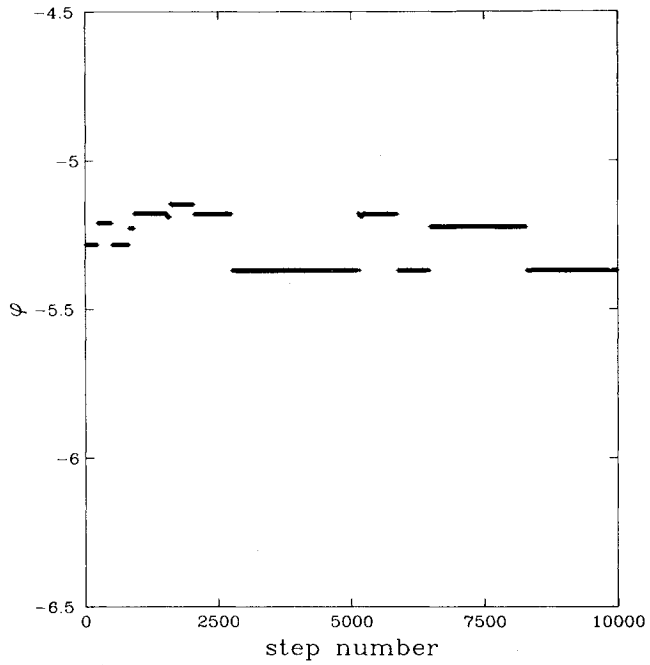

FIG. 5. Amorphous state of the 32-particle system obtained by supercooling to $T=0.773$. Quenches have been constructed every ten time steps.

we infer that the effective mean barrier that must be surmounted is

$$\Delta\Phi=2.16 \ . \tag{3.6}$$

IV. 108-PARTICLE SYSTEM

The number of distinct ϕ values that could be encountered during quenching of this larger system can be estimated from the value of ν shown in Eq. (3.4) above:

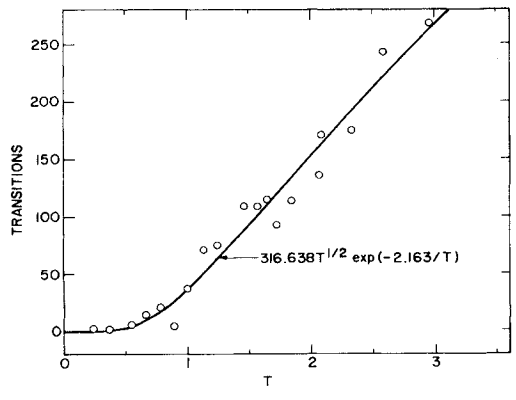

FIG. 6. Numbers of transitions between distinct quench-ϕ values detected during 10^4-step runs for the 32-particle system. Quenches were carried out every ten time steps for all cases shown. Smooth curve shows results from a nonlinear least-squares fit.

$$\exp(\nu N) \simeq \exp(0.16 \times 108)$$
$$\simeq 3.2 \times 10^{7} . \quad (4.1)$$

It is out of the question to create a catalog of such a large number of geometrically distinguishable packings. Nevertheless, selected statistical features of this family of inherent structures is accessible to computation.

Not only does the number Ω of potential minima rise with N, but so too should the rate of transition between the quench regions $\mathscr{R}_\alpha$ surrounding each of those minima. In the large system limit it is sensible to expect that the mean transition rate will be an extensive quantity, i.e., it will be proportional to N. The reason for this expectation is that thermally driven particle rearrangement processes in a large system can occur independently at widely separated locations. By doubling the size of a system (at fixed temperature and density) the number of local rearrangement processes per unit time likewise should double, thereby halving the mean residence time for the system within any given $\mathscr{R}_\alpha$.

Figure 7 shows the quench-ϕ values for a 10^4-step run with the 108 particles at $T=6.46$. This can be compared with the earlier Fig. 3 for the 32 particles at $T=6.44$. In both of these cases the energy is so high (the temperature exceeds three times the melting temperature) that the configuration space is widely sampled during the run, with results shown giving an accurate image of the density distribution of minima along the ϕ axis. The obvious gap in the distribution for 32 particles have now filled in or smoothed out to a large extent. The distribution appears to have its maximum near $\phi=-5.35$, while exhibiting strong skewing toward the low-ϕ side of this maximum.

Figure 8 shows the 108-particle system at the much lower temperature 2.11; this is still within the stable liquid range. Although transitions are less frequent than at the higher temperature the same qualitative view emerges of the distribution of minima with respect to ϕ.

The run depicted in Fig. 8 recorded 780 transitions between distinct quench-ϕ values. The corresponding transition number interpolated from Fig. 6 for the 32-particle system at the same $T=2.11$ is about 165 per 10^4 molecular dynamics steps. Thus the expected increase in transition rate with increasing N is qualitatively achieved, but strict proportionality with N evidently does not apply when N is as small as 32.

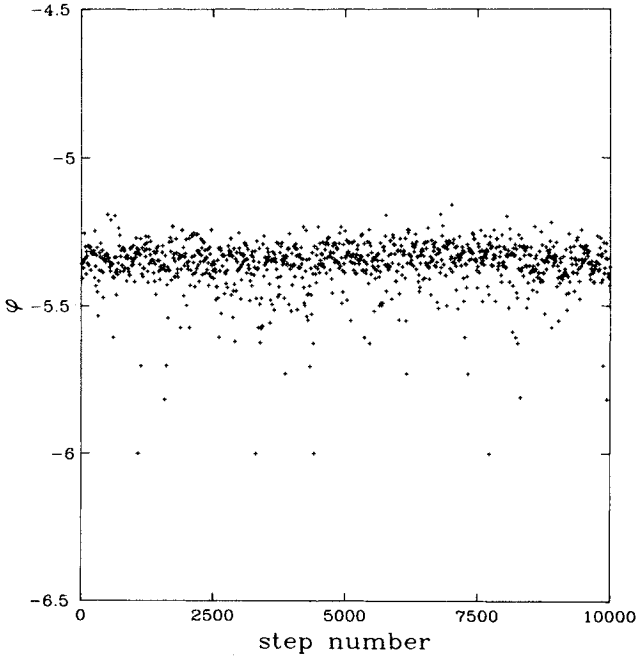

FIG. 7. Quench-ϕ values for the 108-particle system at $T=6.46$, computed every ten time steps.

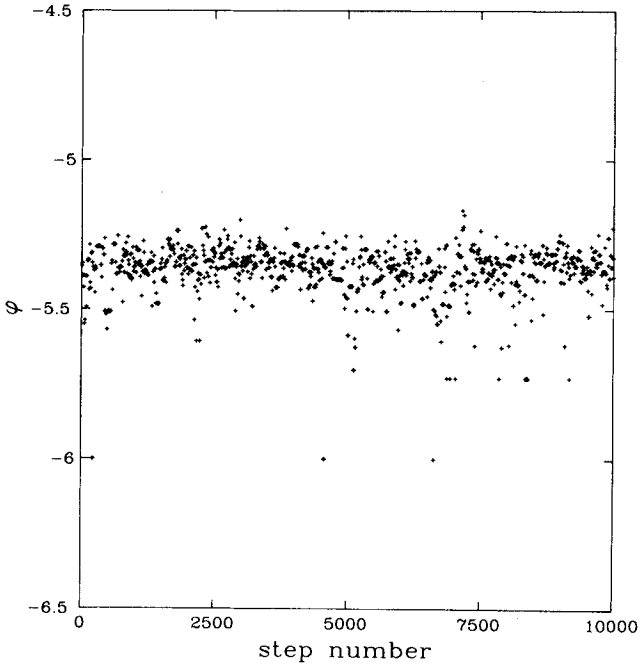

FIG. 8. Quench-ϕ values for the 108-particle system at $T=2.11$, computed every ten time steps.

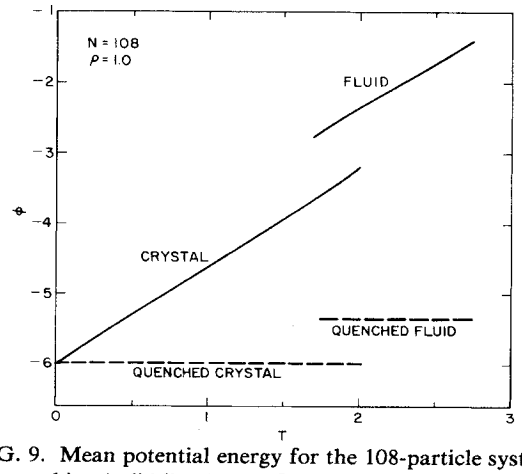

FIG. 9. Mean potential energy for the 108-particle system before quenching (solid lines) and after quenching (dotted lines).

Figure 9 presents (solid lines) thermal average values of ϕ determined during the course of the 108-particle molecular dynamics plotted versus T. The two branches exhibit only minor quantitative differences from those shown in Fig. 1 for the 32-particle system. As N has increased from 32 to 108 the melting temperature appears to have declined from 2.0 to about 1.85.

Figure 9 also presents (dotted lines) the mean values of the ϕ minima encountered as thermodynamic states of the given temperature are subjected to the running quench maps. These are simply time averages accumulated during the dynamical runs generated. While the system is crystalline it invariably quenches to the absolute minimum ϕ. Fluid phases typically produce amorphous quenches whose mean ϕ is about -5.37 near the melting range and is nearly independent of the starting temperature; this means quench ϕ rises only to -5.36 for $T=6.46$. Note should be taken of the fact that at $T=1.85$ the jump of $\Delta\phi=0.63$ between the dotted quench curves only accounts for about 69% of the corresponding jump $\Delta\phi=0.91$ between the solid prequench curves. The remainder must be attributed to the changing extent of anharmonicity that is brought about by the melting process.

Just as was the case with the smaller system, the 108-particle system can be supercooled into a rigid amorphous state. Figure 10 shows both the oscillatory prequench potential energy, and the corresponding quench-ϕ values for a 10^4-step run at $T=0.213$. Three distinct potential minima arise

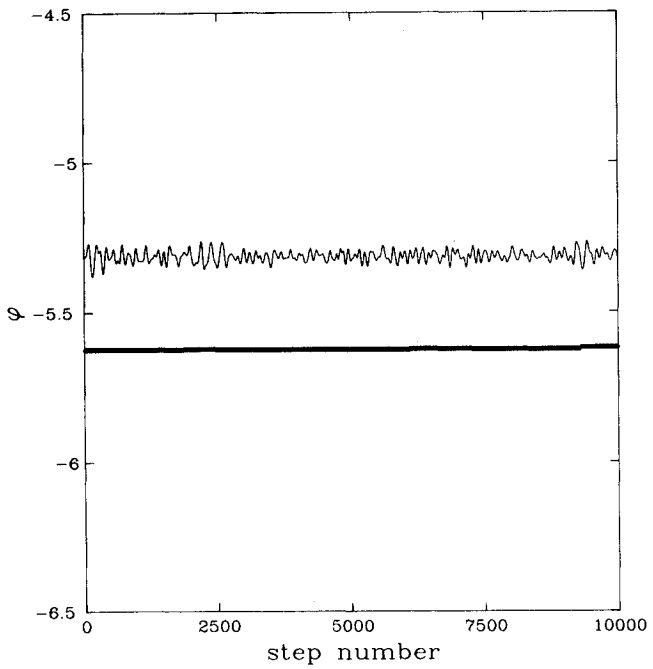

FIG. 10. Potential energy per particle vs time for the 108-particle system in a supercooled amorphous state at $T=0.213$. Upper curve, potential per particle during the Newtonian dynamical motion. Lower curve, quench-ϕ values computed every ten time steps.

$$A:\ \phi=-5.624\,055\ ,$$
$$B:\ \phi=-5.622\,351\ , \tag{4.2}$$
$$C:\ \phi=-5.619\,199\ .$$

They occur in the sequence A,B,A,B,A,C (five transitions), but are barely distinguishable in Fig. 10. Figure 11 provides a vertically expanded view of the quench-ϕ values which make those transitions clearer. The alternation between A and B at the beginning of the dynamical sequence is suggestive of the presence of at least one localized "two-level" system in the medium (a bistable, low-barrier degree of freedom). Such two-level systems, when suitably quantized, are thought to play an important role in many low-temperature properties of amorphous materials.[9,10] We have also observed two-level transitions with different spacings in other low-temperature amorphous states.

Sequences of quench-ϕ values produced during molecular dynamics runs are entirely insensitive to the possible presence of particle permutations. It is conceivable, for instance, that interspersed between the five transitions shown in Fig. 11 are others which merely interchange particles, say by concerted motion along a closed loop. In order to detect the presence of such transitions it suffices to monitor an unsymmetric function of the particle positions at the potential minima. We have employed the following function:

$$Q=\sum_{i=2}^{N}\sum_{j=1}^{i-1}\{[\tfrac{1}{2}(i-1)(i-2)+j]r_{ij}\}\ , \tag{4.3}$$

where the r_{ij} are the particle pair distances in the quenched configuration of interest, always using the minimum-image convention. By this means we have found that direct permutational transitions between

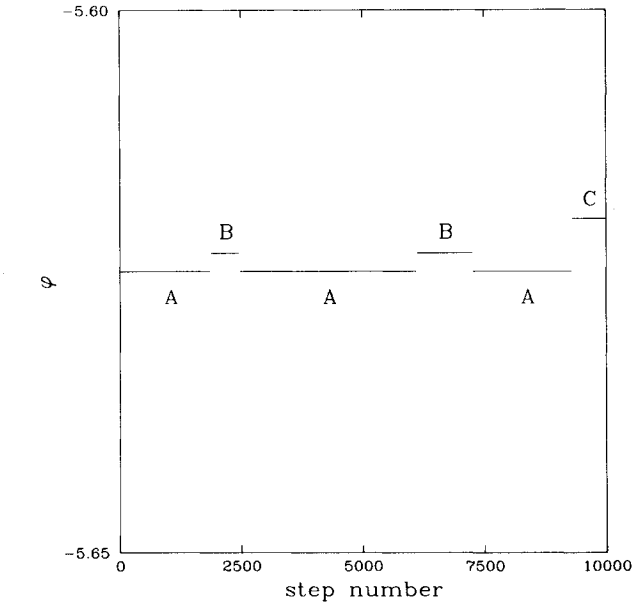

FIG. 11. Quench-ϕ values from Fig. 10 exhibited on a vertically expanded scale.

equivalent potential minima do not occur in strongly supercooled amorphous states. While they have occasionally been detected in the equilibrium fluid near its freezing point, they appear always to constitute a small percentage of transitions.

When transition kinetics is examined closely in the fluid state, a pattern of intermittency often appears. This feature is most clearly evident when the fluid is supercooled to a moderate extent so that the kinetic processes are conveniently slowed down, but not so strongly supercooled that diffusion ceases. Figure 12 shows the quench-ϕ values for a short span of 250 time steps for a supercooled state at $T=1.414$, where now the quenching has been carried out at *every* time step. Figure 13 provides the corresponding smooth and continuous dynamical potential energy. At the beginning of the interval shown in Fig. 12, at a short interval around step 200, and at the end of the sequence, there appear chaotic bursts of changing quench-ϕ values that often switch at every time step. In between these bursts of activity occur relatively quiescent periods, with rather long stretches of residence in the same quench region. Evidently the Newtonian dynamics carries the system through regions which contain closely intertwined "drainage ditches" that descend respectively toward many different potential minima. These peculiar regions have no obvious effect on the dynamical potential energy (cf. Fig. 13). The differential geometry of these chaos-producing multiple-drainage neighborhoods may entail extrema of the monkey-saddle type, i.e., many negative curvature directions. If passage through these regions is important to relaxation and diffusion processes in the fluid, then entropy of activation would necessarily be large. We note in this connection that rate processes in glass-forming liquids can often be fitted to an equation of the Fulcher or VTF form,[11] and that this non-Arrhenius form implies diverging entropy of activation as temperature declines.

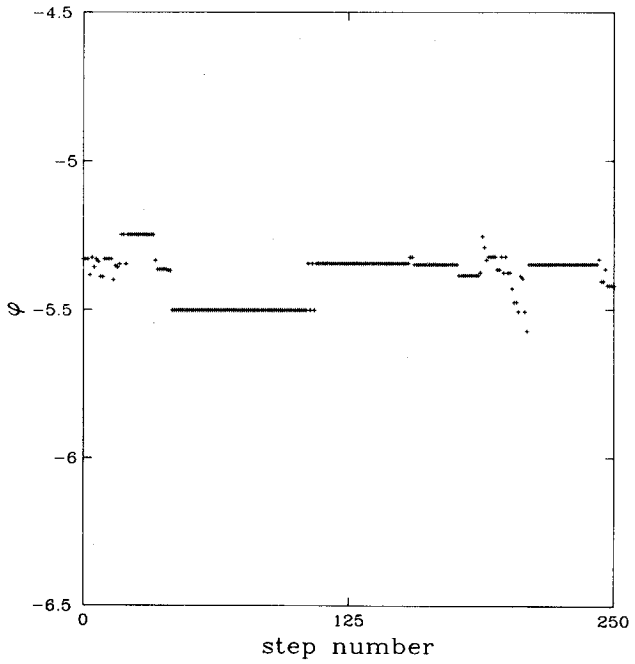

FIG. 12. Quench-ϕ values computed at every time step for the 108-particle system in a supercooled fluid state at $T=1.414$.

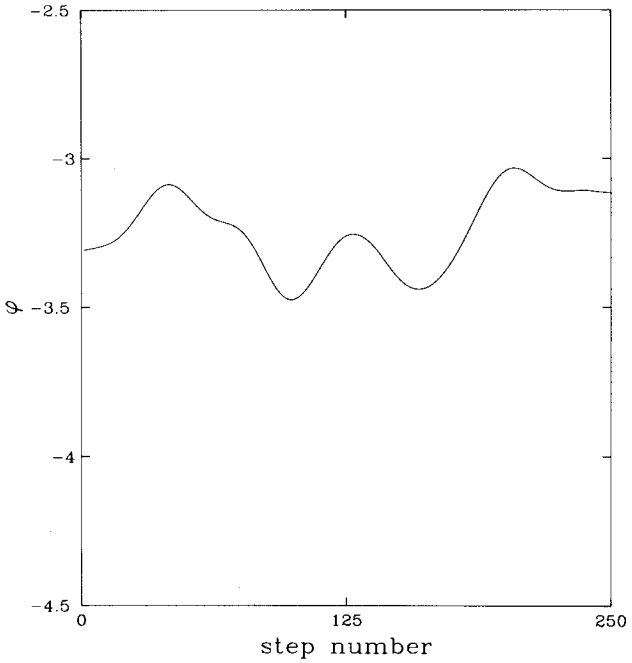

FIG. 13. Potential energy per particle vs time during the Newtonian dynamics for which Fig. 12 gives the corresponding quench-ϕ values.

Let α and β denote a pair of inherent structures that appear one after the other during the quench mapping of the Newtonian dynamics. Furthermore let $\vec{r}_i^{(\alpha)}$ and $\vec{r}_i^{(\beta)}$ be the coordinates of particle i in the corresponding structures. The geometrical change in the particle packing involved in the transition from α to β can be described in terms of displacement vectors $\vec{u}_i$ for each particle:

$$\vec{u}_i=\vec{r}_i^{(\beta)}-\vec{r}_i^{(\alpha)}-\vec{s} \ . \tag{4.4}$$

Here $\vec{s}$ is a translation vector that brings the centroids of the two sets of structures into coincidence, and which thus has the property that it minimizes the sum of squares of displacements

$$\sum_{i=1}^{N} \vec{u}_i^{\,2}=\min \ . \tag{4.5}$$

These sets of displacements have been computed for transitions occurring during a few short molecular dynamics runs with the 108-particle system.

It is useful to compare the sets of displacements with a Gaussian distribution, for which characteristic moment ratios can be evaluated easily, such as

$$\langle \vec{u}^{\,4}\rangle / \langle \vec{u}^{\,2}\rangle^2=\tfrac{5}{3} \tag{4.6}$$

(Gaussian distribution). When the same ratio is evaluated for the transition displacements in the 108-particle system the results usually exceed $\frac{5}{3}$, and typically lie in the range

1.8 to 3.0. Occasionally much larger values arise. This tendency toward large magnitudes of the moment ratio is characteristic of displacements localized on a small subset of particles, i.e., the rearrangement mainly effects only a small group of particles within an essentially rigid host matrix.

Figure 14 illustrates an extreme example of transition localization, occurring during the dynamics of an amorphous state at temperature $T=0.881$. As Fig. 14 indicates, the transition involved a momentary oscillation between the two quench-ϕ values -5.7295 and -5.7043, formally producing three transitions in all. Each of these switches in inherent structure gives rise to

$$\langle \vec{u}^{\,2}\rangle = 0.013988\ ,$$
$$\langle \vec{u}^{\,4}\rangle = 0.010632\ , \tag{4.7}$$
$$\langle \vec{u}^{\,4}\rangle / \langle \vec{u}^{\,2}\rangle^2 = 54.34\ .$$

These are the values to be expected if two particles each move the same distance $\simeq 0.87$, all others remaining fixed, as in rotation or translation of a nearest-neighbor pair. Examination of the relative distance of the pair of particles which have the greatest displacements for the transitions shown reveals that this interpretation is correct.

From the limited studies carried out thus far it has been our impression that the lower the temperature the more localized the particle rearrangements between successively visited inherent structures tend to be. However, further work is needed on this aspect of the problem before firm conclusions can be formulated.

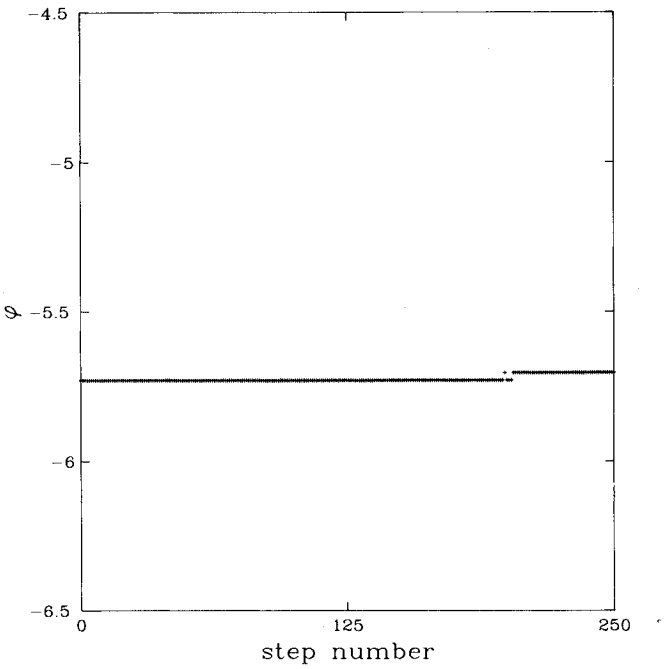

FIG. 14. Quench-ϕ values computed every time step for the 108-particle system in an amorphous state at $T=0.881$.

V. DISCUSSION

The principal conclusions to emerge from this study are the following:

(1) Our model argonlike system exhibits a diverse set of inherent structures which include the crystalline arrangement, but the vast majority of which are amorphous packings.

(2) Transitions between distinct regions corresponding to different inherent structures occur rapidly in the stable liquid phase.

(3) Transition rates rise with temperature, and are probably extensive properties (i.e., proportional to N) in the large system limit.

(4) Permutational transitions are rare.

(5) Localized two-level transitions for bistable, low-barrier degrees of freedom appear prominently in amorphous states at temperatures sufficiently low that self diffusion ceases.

(6) Patterns of intermittency in the quench-ϕ plots occur particularly with low-temperature fluids, suggesting connection to non-Arrhenius behavior of rate processes involving matter transport (self-diffusion, viscosity).

Obviously the dynamics of transition between inherent structures is a complex subject even for "simple" monatomic substances. Many questions remain, such as the precise effects of system size and shape, the influence of variations in the pair potential, and the role of variable density. In regards to the transitions themselves it will be important to locate saddle-point configurations between neighboring quench regions, to compute their height distributions, and to identify the types of "reaction coordinates" which specify the direction of principal negative curvature for each.

The general approach advocated above suggests an exciting opportunity, namely application to covalent and to network-forming liquids, which possess nonadditive and highly directional interactions. The tetrahedral semiconductors silicon and germanium offer important examples, where coordination number 4 in the crystals appears to increase only modestly upon melting.[12] No doubt the amorphous structures these substances form display a great geometric diversity. Our technique offers a means for generating those structures, examining their distribution in potential energy, and securing an understanding of their interconversions.

[1]F. H. Stillinger and T. A. Weber, Kinam 3A, 159 (1981).
[2]F. H. Stillinger and T. A. Weber, Phys. Rev. A 25, 978 (1982).
[3]F. H. Stillinger and T. A. Weber, J. Phys. Chem. (in press).
[4]A. Rahman, Phys. Rev. 136, 405 (1964).
[5]A. Rahman, M. J. Mandell, and J. P. McTague, J. Chem. Phys. 64, 1564 (1976).
[6]S. R. Nagel, A. Rahman, and G. S. Grest, Phys. Rev. Lett. 47, 1665 (1981).
[7]C. W. Gear, Argonne National Laboratory Report No. ANL-7126 (unpublished).

[8]R. Fletcher, *Practical Methods of Optimization* (Wiley, New York, 1980).
[9]P. W. Anderson, B. I. Halperin, and C. M. Varma, Philos. Mag. 25, 1 (1972).
[10]*Amorphous Solids: Low-Temperature Properties,* edited by W. A. Phillips (Springer, Berlin, 1981).
[11]C. A. Angell, Ann. N.Y. Acad. Sci. 371, 136 (1981).
[12]Y. Waseda and K. Suzuki, Z. Phys. B 20, 339 (1975).